Tarig Projected Differential Transform Method for Solving Time-Fractional Gas Dynamics Equation

Athira K, and Narsimhulu D, *Member, IAENG*

Abstract—**A study on the investigation of numerical solutions for two homogeneous nonlinear time-fractional gas dynamics equations (TFGDEs) using an innovative hybrid approach, the Tarig Projected Differential Transform Method (TPDTM), have been analyzed. The new TPDTM simplifies computations easier. This method significantly advantages itself by efficiently handling nonlinear terms through the projected differential transform, thereby eliminating the need for Adomian's and He's polynomials. By combining the Tarig transform with the Projected Differential Transform Method (PDTM), we establish key properties, including linearity, a convolution theorem, and the existence of solutions. Using TPDTM, we found the convergence and stability through absolute error analysis, demonstrating its high accuracy, efficiency, and reliability. To authenticate these findings, a comprehensive comparative analysis is conducted against established numerical methods, namely the Laplace Adomian Decomposition Method (LADM), Finite Difference Method (FDM), Homotopy Perturbation Method (HPM), and Finite Element Method (FEM). The results are presented in tabular and graphical (2D and 3D) formats, highlight TPDTM's superior computational performance. Notably, the solutions obtained from TPDTM and LADM exhibit strong consistency and uniformity, with TPDTM offering a simplified approach to handling Adomian polynomials in LADM. Through two illustrative numerical tests examples, TPDTM demonstrates enhanced computational efficiency and flexibility compared to FDM, LADM, HPM, and FEM, emphasizing its potential as a robust tool for addressing nonlinear fractional differential equations with high accuracy and reliability. The performance of proposed method has been verified using polar and convergence plots, with numerical simulations in MATLAB software.**

***Index Terms*— approximate solution, fractional calculus, gas dynamics equation, numerical methods, tarig projected differential transform technique**

1 Introduction

Gas dynamics (GD) is crucial in the design and development of devices, engines, and gas-powered vehicles, as it provides insights into the forces-such as the body or duct in contact with gas is influenced by several factors, including pressure, temperature, friction, and heat flow. Mathematical modeling is indispensable for predicting and understanding the behavior of these systems and phenomena. Researchers developed various methods to derive approximate and analytical solutions for homogeneous and nonhomogeneous TFGDEs. Several prominent researchers in this field include the work of Jafari et al. [1], Kumar et al. [2], Mohamed et al. [3], Al-luhaibi [4], Esen et al. [5], and Tamsir and Srivastava [6]. To efficiently analyze and solve GD equations, these researches used a variety of numerical and semi-analytical approaches, such as the HPM, Homotopy Analysis Transform Method (HATM), New Iteration Method (NIM), FDM and Reduced Differential Transform Method (RDTM).

The recent work reports in the field of fractional calculus were led to the development of diverse methodologies for solving fractional GD equations (FGDEs). The Reproducing Kernel Hilbert Space Method (RKHSM) was used to solve the nonhomogeneous FGDEs by Akgul et al. [7]. Jassim and Mohammed [8] integrated the Natural Transform (NT) with HPM to explore solutions for nonlinear FGDEs. Iyanda [9] introduced a Modified Iterative Method (MIM) to obtained numerical solutions for nonlinear FGDEs. Alaroud et al. [10] proposed the Laplace Residual Power Series Method (LRPSM), an innovative analytical, for solving nonlinear TFGDEs. Additionally, Jebreen and Cattani [11] employed a Collocation Method based on Muntz-Legendre polynomials, (CM M-L), representing the unknown solution allowing for flexible and accurate approximation of the solution.

Recently, the authors Yousif et al. [12] and Sadaf et

Manuscript received October 31, 2024; July 11, 2025.

This work was supported in part by the University Grant Commission (UGC), New Delhi, India, through the Savitribai Jyotirao Phule Fellowship for Single Girl Child (SJSGC) [F. NO. 82-7/2022 (SA-III)].

Athira K is a Research Scholar in the Department of Statistics and Applied Mathematics, Central University of Tamil Nadu, Neelakudi, Thiruvarur-610005, Tamil Nadu, India (e-mail: aathus25@gmail.com).

Narsimhulu D is an Assistant Professor in the Department of Statistics and Applied Mathematics, School of Mathematics and Computer Sciences, Central University of Tamil Nadu, Neelakudi, Thiruvarur-610005, Tamil Nadu, India (corresponding author to provide phone: +91-6305422042; e-mail: narsimha.maths@gmail.com).

al. [13] applied the Conformal Finite Difference Method (CFDM) and the Elzaki Decomposition Method (EDM), respectively to derive approximate analytical solutions for both homogeneous and nonhomogeneous TFGDEs. Rabia et al. [14] employed an extended cubic B-spline collocation method incorporating local fading memory via the Caputo-Fabrizio fractional-order differential operator to numerically solve the nonlinear fractional-order GD equation. In 2025, they [15] and [16] employed exponential cubic B-spline and cubic B-spline function to examine the nonlinear fractional-order GD equation incorporating Caputo-fractional, Atangana Baleanu derivatives, respectively.

Several researchers perform comprehensive research investigations on approximate analytical and numerical methods. To solve both the homogeneous and nonhomogeneous nonlinear GD equations [10, 17, 18], the diverse techniques, such as the HPM [19], the fractional Homotopy Analysis Transform Method (HATM) [20], the Differential Transform Method (DTM) [21], the Laplace Homotopy Perturbation Method (LHPM) [22], FDM [23], and Homotopy Analysis Method (HAM) [24] illustrated lucidly. These methodologies demonstrate the diverse strategies employed to address the complexities with GD systems.

For solving GD equations, existing methods will often have some drawbacks and notable limitations, while useful. Computational cost can be a significant issue for methods like HAM, HPM, HATM, KHSM. The LRPSM, and MIM may convergence slowly and low accuracy in some cases. Instability and sensitivity to boundary conditions were analyzed with FDM and CM M-L. Furthermore, the standard methods NIM, DTM, EDM, and CFDM were partially discussed to solve the GD type equations because of potential inaccuracies and numerical instability. These limitations motivate the development of more robust and efficient approaches for tackling many complex problems. This study introduces TPDTM [25], a novel hybrid approach that combines the Tarig transforms [26] with PDTM [27] to solve homogeneous nonlinear TFGDEs.

With aid of PDTM, this technique transforms the fractional derivatives into a series expansion to solve the problem. The PDTM and its advanced variant, the TPDTM, build upon the classical Differential Transform Method (DTM) by incorporating fractional derivatives and customized projection techniques to enhance convergence and computational efficiency. The proposed semi-analytical TPDTM addresses the limitations of the aforementioned traditional methods. This method significantly improves the numerical stability and performance and reduces computational overhead by combining the projection mechanism with the differential framework. The TPDTM offers an efficient solution for solving complex time-fractional partial differential equations (TFPDEs), in particularly those arising in GD.

Rooted in fractional calculus [28], these equations extend classical GD equations by incorporating time-fractional derivatives, enabling the modelling of complex phenomena such as turbulent flow, heat transfer in rarefied gases, and GD behaviors influenced by memory effects and anomalous diffusion. TFGDEs are particularly relevant in scenarios involving shock waves, fractional-order effects, and contact discontinuities, making them essential for understanding intricate GD systems. Athira et al. [32] proposed TPDTM in their research work to solve nonlinear TFPDEs, such as the Newell-Whitehead-Segel (N-W-S) and Burger's equations, demonstrating its superior efficiency, reliability, and stability compared to other established methods in literature. In 2024, Elzaki [33] employed PDTM to derived the solution for non-linear GDEs. To the best of author's investigation, this study presents the first application of the TPDTM to obtain numerical approximate solutions for TFGDEs.

We produce the TPDTM as a robust and efficient method for addressing homogeneous GD equation with various particular non-integer initial and boundary conditions. To validate the present results and assess the computational efficiency of TPDTM, a comprehensive comparative analysis was performed against the solutions obtained using FDM, LADM, HPM, and FEM. Additionally, TPDTM functions effectively without requiring any linearization, perturbation techniques, discretization of variable, or imposing restrictive assumptions. It ensures a high degree of accuracy, is computationally efficient, utilizes minimal memory and time, and effectively handles both linear and nonlinear differential equations without necessitating boundary condition adjustments. Due to its intrinsic stability and ability to control errors while enhancing solution accuracy, TPDTM emerges as a highly effective and adaptive approach, making it a compelling alternative to conventional methods documented in the literature.

The paper follows this structure: Section 2 provides key terminology and the mathematical principles underlying the fractional calculus theory. The application of the proposed method to numerically solve the TFGDEs is detailed in Section 3. Section 4 illustrates and discusses the numerical results. Section 5 concludes the paper, summarizing key insights and findings. This structure provides a clear and logical flow, guiding the reader through the theoretical underpinnings, methodology, results, and conclusions of the study.

2 Methodology

The choice of a fractional derivative determines the mathematical structure and physical fidelity of a system, playing a critical role in extending models to capture complex phenomena accurately [14, 16, 34]. Various definitions — "Caputo, Riemann-Liouville, Riesz, Caputo-Fabrizio, Atangana-Baleanu, and Grunwald-Letnikov" — address different modeling needs. Samko et al. [29] provide a thorough mathematical basis for fractional calcu-

lus, offering various definitions and properties. Caputo [30] introduces the Caputo fractional derivative, modifying the traditional Riemann-Liouville definition for improved handling of initial conditions in physical problems. From this, the definitions required for this study are discussed below.

2.1 Basic Definitions

This section provides fundamental definitions as follows:

Definition 1. [29] Let function $f(t) \in L_1(a,b)$ and $\alpha > 0$. Then the fractional integral under Reimann-Liouville framework of order α from

a) left-sided for $f(t)$ defined as:

$$\left(I^{\alpha}_{a^+} f\right)(t) = \frac{\int_a^{\infty} (t-s)^{\alpha-1} f(s)\, ds}{\Gamma(\alpha)}, \quad s > \alpha.$$

b) right-sided for $f(t)$ defined as:

$$\left(I^{\alpha}_{b^-} f\right)(t) = \frac{\int_{-\infty}^{b} f(s)(t-s)^{\alpha-1}\, ds}{\Gamma(\alpha)}, \quad s < \alpha.$$

Definition 2. [29] One can define the Riemann integral with a variable limit on the half axis as follows

$$\left[I^{\alpha}_{0^+} f\right](t) = \frac{\int_a^{\infty} (t-s)^{\alpha-1} f(s)\, ds}{\Gamma(\alpha)}, \quad 0 < t < \infty.$$

Definition 3. [29] The Reimann-Liouville derivative of fractional order α, $\alpha \in (0,1)$ in the interval $[a,b]$ of

a) left-sided for $f(t)$ is given as

$$\left(D^{\alpha}_{a^+} f\right)(t) = \frac{\frac{d}{dt}[\int_a^t (t-s)^{-\alpha} f(s)\, ds].}{\Gamma(1-\alpha)}$$

b) right-sided for a function $f(t)$ defined as

$$\left(D^{\alpha}_{b^-} f\right)(t) = \frac{\frac{d}{dt}[\int_t^b (t-s)^{-\alpha} f(s)\, ds].}{\Gamma(1-\alpha)}$$

Definition 4. [30] The Caputo definition defines the fractional derivative of $f(t)$ for $\alpha \in (n-1, n]$, $t > 0$ and n belongs to N by

$$D^{\alpha} f(t)\Gamma(n-\alpha) = \int_0^t f^{(n)}(s)(t-s)^{-(\alpha+1)+n}\, ds.$$

Definition 5. [31] The Mittag-Leffler function, is defined for $\alpha \in C$,
$Re(\alpha) > 0$, by $E_{\alpha}(Z) = \sum_{n=0}^{\infty} \frac{Z^n}{\Gamma(n\alpha+1)}$

2.2 Tarig Transform

The definition of the Tarig transforms of a temporal function, $f(t)$ is given by [26]:

$$T[f(t)] = \frac{\int_0^{\infty} e^{-\frac{t}{\vartheta^2}} f(t)\, dt}{\vartheta}, \quad \vartheta \neq 0, \tag{1}$$

where ϑ serves as a frequency variable.
Let $f(t)$ is the temporal function, its corresponding frequency space function representation through the Tarig transform of order α is denoted by $F(\vartheta)$. Then, the fractional integral of $f(t)$ under the Tarig transform framework for order α [26] is:

$$T\left[(I^{\alpha}_{0^+} f)(t)\right] = \vartheta^{2\alpha} F(\vartheta) = \vartheta^{2\alpha} T[f(t)]. \tag{2}$$

In a similar manner, the fractional derivative of $f(t)$ of order α under the Tarig transform framework [25] is given by:

$$F^{\alpha}(\vartheta) = T\left[D^{\alpha} f(t)\right]$$
$$\frac{F(\vartheta)}{\vartheta^{2\alpha}} - \sum_{i=1}^{n} \vartheta^{2(i-\alpha)-1} f^{(i-1)}(0). \tag{3}$$

2.3 Definition, Property and Theorem of PDTM

If $f(X)$, with $X = (x_1, x_2, \ldots, x_n)$ is a multivariable function. Define $X_{[n-1]} = (x_1, x_2, \ldots, x_{n-1})$. Then PDTM of $f(X_{[n-1]}, k)$ [27] as:

$$f(X_{[n-1]}, k) = \frac{1}{k!}\left[\frac{\partial^k f(X)}{\partial x_n^k}\right]_{x_n}, \tag{4}$$

here $f(X_{[n-1]}, k)$ is PDT function of original function $f(X)$.
The differential inverse transform of $f(X_{[n-1]}, k)$ can be defined [27] as follows:

$$f(X) = \sum_{k=0}^{\infty} f(X_{[n-1]}, k)\,(x - x_0)^k. \tag{5}$$

Now, we present some basic theorems [27]of the PDTM that are relevant to this work.
Condider two multi variable functions $u(X)$ and $v(X)$ with $u(X_{[n-1]}, k)$ and $v(X_{[n-1]}, k)$ are PDT functions of u and v respectively.
Consider c as a constant.

- If $z(X) = u(X)v(X)$, then $z(X_{[n-1]}, k) = u(X_{[n-1]}, k)v(X_{[n-1]}, k)$.
- If $z(X) = cu(X)$, then $z(X_{[n-1]}, k) = cu(X_{[n-1]}, k)$.
- If $z(X) = \frac{d^n u(X)}{(dx_n^n)}$, then $z(X_{[n-1]}, k) = \frac{(k+n)}{k!} u(X_{[n-1]}, k+n)$.
- If $z(X) = u(X)v(X)$, then $z(X_{[n-1]}, k) = \sum_{m=0}^{k} u(X_{[n-1]}, m)v(X_{[n-1]}, m)$.
- If $z(X) = u_1(X)u_2(X)...u_n(X)$, then $z(X_{[n-1]}, k) =$

$$\sum_{k_{n-1}=0}^{k} \sum_{k_{n-2}=0}^{k_{n-1}} \cdots \sum_{k_2=0}^{k_3} \sum_{k_1=0}^{k_2} u_1(X_{[n-1]}, k_1)$$

$$u_2(X_{[n-1]}, k_2 - k_1)...u_{n-1}(X_{[n-1]}, k_{n-1} - k_{n-2})$$
$$u_n(X_{[n-1]}, k_n - k_{n-1}).$$

2.4 TPDTM Methodology

Consider the nonlinear TF PDE:

$$(D^\alpha + R + N)U(x,t) = g(x,t), \tag{6}$$

subjected to the rudimentary:

$$U(x,0) = f(x). \tag{7}$$

where $D^\alpha = \frac{\partial^\alpha}{\partial \tau^\alpha}$ is the fractional derivative operator of order α, where $g(x,t)$ represents the source term, R and N correspond to linear and nonlinear differential operators, respectively [32].
By operating the Tarig transform on Eq.(6), we derive [32]

$$T[(D^\alpha + R + N)U(x,t)] = T[g(x,t)]. \tag{8}$$

Using the differential property of the Tarig transform given in Eq. (3) of the Tarig transform on Eq.(6) and (7), we obtain [25]:

$$T[D^\alpha U(x,t)] = \vartheta f(x) + \vartheta^{2\alpha}(T[g(x,t) - (R+N)U(x,t)]). \tag{9}$$

Inverting the Tarig transform to the Eq. (9) and using the fact that $T^{-1}(\vartheta) = 1$, we obtain [32]

$$U(x,t) = G(x,t) - T^{-1}[\vartheta^{2\alpha}(T[(R+N)U(x,t)])] \tag{10}$$

where $G(x,t)$ denoted the term arise from the rudimentary and the source term.
Using PDTM, the Eq. (10) reduces as [25]

$$U(x,m+1) = -T^{-1}[\vartheta^{2\alpha}(T[(R+N)U(x,t)])]. \tag{11}$$

where $m \geq 0, U(x,0) = f(x)$
The closed form of solution for Eq. (6) and (7) takes the form of the series:

$$U(x,t) = U(x,0) + U(x,1) + U(x,2) + ..., \tag{12}$$

where each function $U(x,m), m = 0$ to ∞ are in terms of x and t only.

2.5 Linearity property of TPDTM:

We consider two functions $f(t)$ and $g(t)$, then $T[D^\alpha(af(t) + bg(t))] = aT[D^\alpha f(t)] + bT[D^\alpha g(t)]$, where a and b serves as a constants.
Proof: Let $F(\vartheta)$ and $G(\vartheta)$ be the Tarig transforms of $f(t)$ and $g(t)$ respectively.
Using the differential property given in Eq. (3) of the Tarig transform,

$$T\left[D^\alpha(af(t) + bg(t))\right] = \frac{(aF + bG)(\vartheta)}{\vartheta^{2\alpha}} -$$
$$\sum_{i=1}^{n} \vartheta^{2(i-\alpha)-1} \left(af + bg\right)^{(i-1)}(0).$$
$$= \frac{1}{\vartheta^{2\alpha}}[aF(\vartheta) + bG(\vartheta)] -$$
$$\sum_{i=1}^{n} \vartheta^{2(i-\alpha)-1} \left(af^{(i-1)}(0) + bg^{(i-1)}(0)\right).$$
$$= a\frac{F(\vartheta)}{\vartheta^{2\alpha}} + b\frac{G(\vartheta)}{\vartheta^{2\alpha}} - a\sum_{i=1}^{n} \vartheta^{2(i-\alpha)-1} f^{(i-1)}(0) -$$
$$b\sum_{i=1}^{n} \vartheta^{2(i-\alpha)-1} g^{(i-1)}(0).$$

Since PDTM holds linearity, after rearranging terms in the above expression, we get

$$T[D^\alpha(af(t) + bg(t))] = aT[D^\alpha f(t)] + bT[D^\alpha g(t)]$$

2.6 TPDTM Convolution theorem:

The convolution of two functions $f(t)$ and $g(t)$ of fractional order α is given by
$(f * g)_\alpha(t) = \int_0^\infty f(t-\tau)g(\tau)\,(d\tau)^\alpha$,
and then the convolution of TPDTM of fractional order α is given by

$$T\left[D^\alpha(f * g)_\alpha(t)\right] = \frac{F_\vartheta(\vartheta)G_\vartheta(\vartheta)}{\vartheta^\alpha} - Z,$$

where

$$Z = \sum_{i=1}^{n}\sum_{j=0}^{i-2} \vartheta^{2(i-\alpha)-1} f^{(j)}(0)\, g^{(i-j-2)}(0),$$

is the correction term.
Proof: Using the differential property of the Tarig transform given in Eq. (3)

$$T\left[D^\alpha(f * g)(t)\right] = \frac{(F * G)(\vartheta)}{\vartheta^{2\alpha}} -$$
$$\sum_{i=1}^{n} \vartheta^{2(i-\alpha)-1}(f * g)_\alpha^{(i-1)}(0).$$

Since, convolution theorem of the Tarig transform is $T[(f * g)(t)] = (F * G)(\vartheta) = \vartheta^\alpha F_\alpha(\vartheta)G_\alpha(\vartheta)$, where

$$F_\alpha(\vartheta) = \frac{H_\alpha\left(\frac{1}{\vartheta^2}\right)}{\vartheta^\alpha}$$

and

$$G_\alpha(\vartheta) = \frac{W_\alpha\left(\frac{1}{\vartheta^2}\right)}{\vartheta^\alpha}$$

where H_α and W_α related to the Laplace transform [31]. This implies

$$T\left[D^\alpha(f * g)_\alpha(t)\right] = \frac{\vartheta^\alpha}{\vartheta^{2\alpha}} F_\alpha(\vartheta)G_\alpha(\vartheta) -$$

$$\sum_{i=1}^{n} \vartheta^{2(i-\alpha)-1} (f*g)_{\alpha}^{(i-1)}(0).$$

Since, the convolution of f and g are $(f*g)_{\alpha}(t) = \int_0^{\infty} f(t-\tau)g(\tau)\,(d\tau)^{\alpha}$, implies

$$T\left[D^{\alpha}(f*g)_{\alpha}(t)\right] = \frac{1}{\vartheta^{\alpha}} F_{\alpha}(\vartheta) G_{\alpha}(\vartheta) -$$

$$\sum_{i=1}^{n} \sum_{j=0}^{i-2} \vartheta^{2(i-\alpha)-1} f^{(j)}(0)\, g^{(i-j-2)}(0),$$

Ie,

$$T\left[D^{\alpha}(f*g)_{\alpha}(t)\right] = \frac{1}{\vartheta^{\alpha}} F_{\alpha}(\vartheta) G_{\alpha}(\vartheta) - Z,$$

where

$$Z = \sum_{i=1}^{n} \sum_{j=0}^{i-2} \vartheta^{2(i-\alpha)-1} f^{(j)}(0)\, g^{(i-j-2)}(0)$$

is the correction term depends on the specific characteristics of the problem (e.g., initial condition and fractional order α).

2.7 Theorem: Existence of solutions for the TPDTM

If $f(t) \in A$ is sectionally continuous in every finite interval $0 \le t \le n$ and is continuously differentiable in A, where

$$A = \left\{ f(t) : \exists M, n_1, n_2 > 0, |f(t) < M e^{\frac{|t|}{k_j}}|, t \in (-1)^j \times [0, \infty) \right\}$$

and of exponential order β, for $t > n$, then the existence of the solution of TPDTM of the TFPDE of order α, $D^{\alpha} f(t)$ with initial condition $f(0)$, happens under the following conditions:
(1)The Tarig transform $F(\vartheta)$ of $f(t)$ exists for all $\vartheta > \beta$. (existence of solution of Tarig transform) [31].
(2) The convergence of nonlinear term in the series form (existence of a solution of PDTM) guarantees the existence of a solution of TPDTM.
Proof: By using the differential property given in Eq. (3),

$$T\left[D^{\alpha} f(t)\right] = F^{\alpha}(\vartheta) = \frac{1}{\vartheta^{2\alpha}} F(\vartheta) - \sum_{i=1}^{n} \vartheta^{2(i-\alpha)-1} f^{(i-1)}(0)$$

Since $T[f(t)] = F(\vartheta)$, this implies:

$$T\left[D^{\alpha} f(t)\right] = \frac{1}{\vartheta^{2\alpha}} T[f(t)] - \sum_{i=1}^{n} \vartheta^{2(i-\alpha)-1} f^{(i-1)}(0)$$

Then, (1) For any positive number n,

$$T[f(t)] = \frac{\int_0^{\infty} f(t)\, e^{-\frac{t}{\vartheta^2}} dt}{\vartheta} =$$

$$\frac{1}{\vartheta} \left[\int_0^{n} f(t)\, e^{-\frac{t}{\vartheta^2}} dt + \int_n^{\infty} f(t)\, e^{-\frac{t}{\vartheta^2}} dt \right] \qquad (13)$$

Since $f(t)$ is sectionally continuous in every finite interval $[0, n]$, then the right side first integral exists. Since $f(t)$ is of exponential order β for $t > n$,

$$\left| \int_n^{\infty} f(t)\, e^{-\frac{t}{\vartheta^2}} dt \right| \le \int_n^{\infty} \left| f(t)\, e^{-\frac{t}{\vartheta^2}} \right| dt$$

$$\le \int_n^{\infty} |f(t)|\, e^{-\frac{t}{\vartheta^2}} dt$$

$$\le \int_n^{\infty} e^{-\frac{t}{\vartheta^2}} M e^{\frac{\beta}{\vartheta^2}} dt = \frac{M\vartheta}{(1-\beta)}, \beta \ne 1$$

which implies the existence of a solution of the Tarig transform.
Implies first term in the Eq. (13) exists.
(2) Since $f(t)$ is continuously differentiable in A, there series term, $\sum_{i=1}^{n} \vartheta^{2(i-\alpha)-1} f^{(i-1)}(0)$, in the second term in RHS of Eq. (13) is well defined.
Using the inverse property of Tarig transform and decomposition of nonlinear term using PDTM, the exact solution is series form obtained as $f(t) = \sum_{m=0}^{\infty} F_m(t) t^m$, where each $F_m(t)$ obtained recursively using PDTM. Since $f(t)$ with respect to the exponential order $\beta > 0$ and $\beta \ne 1$ (by part (1) of the proof) for $t > n$. Then there exists $M > 0$, $|f(t)| \le M\beta^m$ (since each $f(t) \in A$) implies the series $f(t) = \sum_{m=0}^{\infty} F_m(t) t^m$, converges uniformly. Then part (1) and (2) guarantee the existence of a solution of TPDTM.

2.8 Error Calculation and Convergence and Stability of the Method

A thorough convergence analysis is necessary to establish the trustworthiess of the solution in Eq. (12). The approximate numerical solution for the Eq.(6) with (7) can be obtained [25] as

$$U_{app(k)}(x,t) = \sum_{m=0}^{k} U(x,m)$$

By disregarding higher-order term ($m > n$) in the summation in Eq. (12) the exact solution of Eq. (6) and (7) can be obtained [25] as

$$U(x,t) = (U_{app(k)} + e_k U)(x,t)$$

clearly $e_k U(x,t)$ is defined as a error function.
Now, the absolute error can be expressed as

$$e_k U(x,t) = |(U - U_{app(k)})(x,t)|.$$

For the highly practical scenarios, a closed form solution, $U(x,t)$, is not possible. So, the absolute error associated with the approximate numerical solution [25] is

$$E_k U(x,t) = |(U_{app(k)} - U_{app(k+1)})(x,t)|. \qquad (14)$$

Demonstrating convergence for equation (12) necessary to prove that $\{E_k U(x,t)\}$ is convergent. As this sequence

$\{E_kU(x,t)\}$ has a lower bound, establishing its monotonic decreasing nature would suffice to guarantee convergence. Hence, the convergence criteria [25] is $\left|\frac{E_pU(x,t)}{E_kU(x,t)}\right| < 1$ for $k < p$.
To establish the convergence, the iterative approximation $U_{app(k)}(x,t)$ to the closed form solution $U(x,t)$ involves the following 4 steps [25].

1. Determine $U_{app(k)}(x,t)$, $U_{app(k+1)}(x,t)$
2. Determine $U_{app(p)}(x,t)$, $U_{app(p+1)}(x,t), k \leq p$
3. Delineate
   $E_kU(x,t) = |U_{app(k)}(x,t) - U_{app(k+1)}(x,t)|$,
   $E_pU(x,t) = |U_{app(p)}(x,t) - U_{app(p+1)}(x,t)|$ for some x and t.
4. If $E_kU(x,t) \geq E_pU(x,t)$, then $U_{app(k)}(x,t)$ converges to the closed form solution $U(x,t)$ when $k \to \infty$

This algorithm is applied in this paper to prove the convergence of the series solution obtained by TPDTM. If the series converges, then it is stable.

3 Numerical Test Examples

Test Example 1. We assume the homogenous TFGDE

$$D^\alpha U + UU_x - U(1-U) = 0, \alpha \in (0,1]. \quad (15)$$

subjected to the rudimentary:

$$U(x,0) = e^{-x}. \quad (16)$$

Apply Tarig transform in Eq. (15), with initial condition given in Eq. (16) and using the differential property given in Eq. (3) of the Tarig transform, we obtain

$$T[U(x,t)] - \vartheta e^{-x} = -\vartheta^{2\alpha}[T[UU_x - U(1-U)]] \quad (17)$$

Inverting the Tarig transform to the Eq. (17) and using the fact that $T^{-1}(\vartheta) = 1$, we obtain

$$U(x,t) = e^{-x} - T^{-1}[\vartheta^{2\alpha}[T[UU_x - U(1-U)]]] \quad (18)$$

Using PDTM, Eq. (18) become

$$U(x,m+1) = -T^{-1}[\vartheta^{2\alpha}[T[UU_x - U(1-U)]]],$$
$$m \geq 0, U(x,0) = e^{-x} \quad (19)$$

Based on the Eq. (19), the following expression is obtained:

$$U(x,1) = \frac{e^{-x}t^\alpha}{\Gamma(\alpha+1)}, U(x,2) = \frac{e^{-x}t^{2\alpha}}{\Gamma(2\alpha+1)},$$
$$U(x,3) = \frac{e^{-x}t^{3\alpha}}{\Gamma(3\alpha+1)}, U(x,4) = \frac{e^{-x}t^{4\alpha}}{\Gamma(4\alpha+1)},$$
$$\ldots, U(x,n) = \frac{e^{-x}t^{n\alpha}}{\Gamma(n\alpha+1)}$$

Continuing in the same manner, the subsequent iterations can be obtained accordingly. we get the the remaining iterations.
Therefore, the series of Eqs. (15) and (16) is by TPDTM is given by

$$U(x,t) = U(x,0) + U(x,1) + U(x,2) + ...,$$
$$U(x,t) = e^{-x} + \sum_{k=1}^{\infty} e^{-x}\frac{t^{k\alpha}}{\Gamma(k\alpha+1)}$$

Test Example 2. Consider the homogenous nonlinear TFGDE

$$D^\alpha U + UU_x - U(1-U)loga = 0, 0 < \alpha \leq 1. \quad (20)$$

subjected to the rudimentary:

$$U(x,0) = a^{-x}. \quad (21)$$

Taking Tarig transform on both sides of Eq. (20), with rudimentary given in Eq. (21) and using the differential property given in Eq. (3) of the Tarig transform, we obtain

$$T[U(x,t)] = \vartheta a^{-x} - \vartheta^{2\alpha}[T[(UU_x - U(1-U))loga]] \quad (22)$$

Inverting the Tarig transform to the Eq. (22) and using the fact that $T^{-1}(\vartheta) = 1$, we obtain

$$U(x,t) = a^{-x} - T^{-1}[\vartheta^{2\alpha}[T[(UU_x - U(1-U))loga]]] \quad (23)$$

Using PDTM, the Eq. (23) become

$$U(x,m+1) = -T^{-1}[\vartheta^{2\alpha}[T[(UU_x - U(1-U))loga]]],$$
$$m \geq 0, U(x,0) = a^{-x} \quad (24)$$

Based on the Eq. (24), the following expression is obtained:

$$U(x,1) = \frac{(loga)a^{-x}t^\alpha}{\Gamma(\alpha+1)},$$
$$U(x,2) = \frac{(loga)^2a^{-x}t^{2\alpha}}{\Gamma(2\alpha+1)},$$
$$U(x,3) = \frac{(loga)^3a^{-x}t^{3\alpha}}{\Gamma(3\alpha+1)},$$
$$U(x,4) = \frac{(loga)^4a^{-x}t^{4\alpha}}{\Gamma(4\alpha+1)},$$
$$\ldots, U(x,n) = \frac{(loga)^na^{-x}t^{n\alpha}}{\Gamma(n\alpha+1)}.$$

Continuing in the same manner, the subsequent iterations can be obtained accordingly.
Therefore, the series of Eqs. (20) and (21) is by TPDTM is given by

$$U(x,t) = U(x,0) + U(x,1) + U(x,2) + ...,$$
$$U(x,t) = a^{-x} + \sum_{k=1}^{\infty} a^{-x}\frac{t^{k\alpha}}{\Gamma(k\alpha+1)}(loga)^k.$$

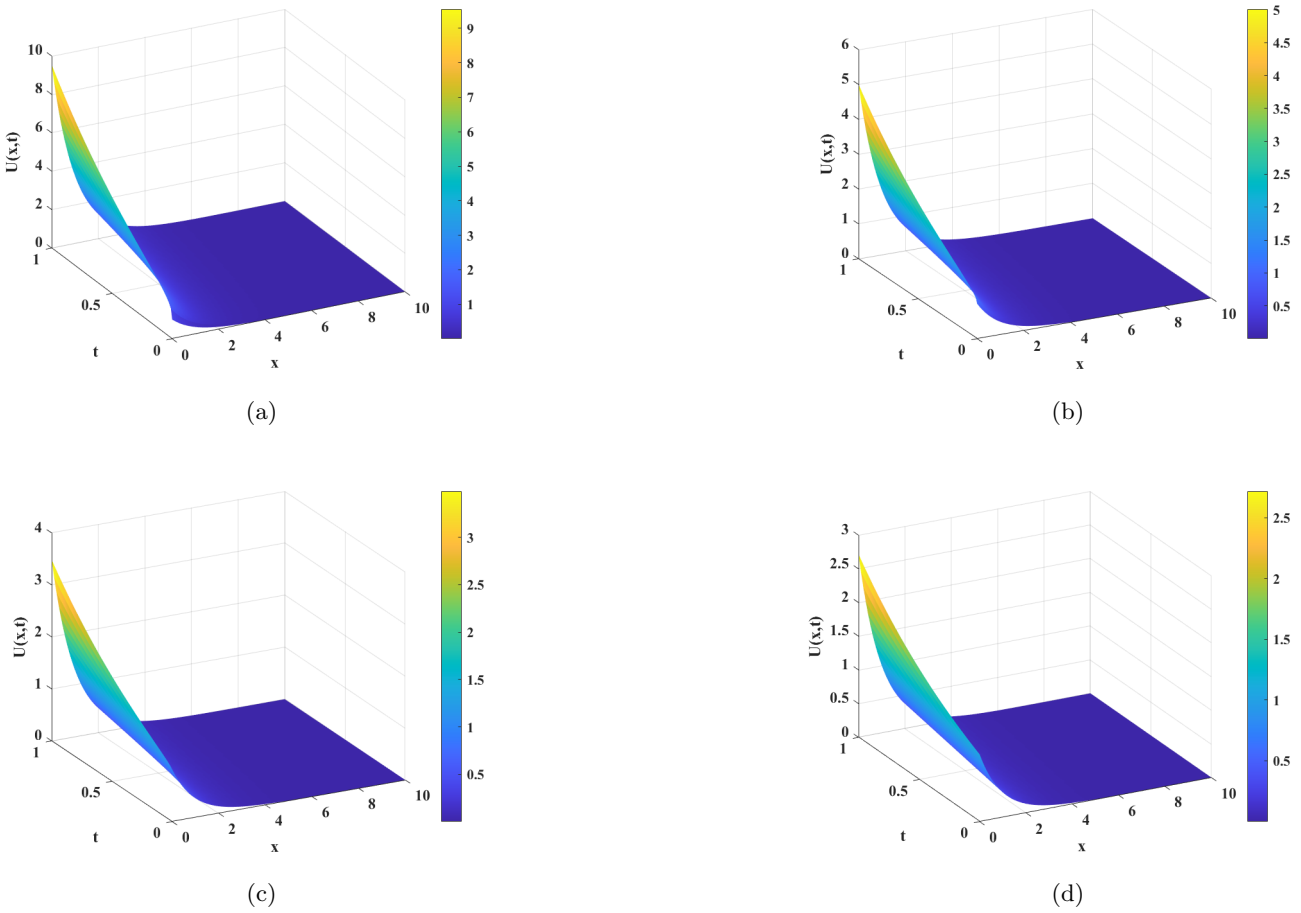

Fig. 1: Analysis of $U(x,t)$ of test example 1 is presented for $\alpha = (0.25, 0.50, 0.75 \text{ and } 1)$ in a, b, c and d respectively using TPDTM.

Table 1: Illustration of $U(x,t)$ of test example 1 for range of α and x when $t = 1$

x-value	$U(x,t)$ with respect to the fractional order α			
	$\alpha = 0.25$	$\alpha = 0.5$	$\alpha = 0.75$	$\alpha = 1$
0	9.5541	5.009	3.4859	2.7183
1	3.5148	1.8427	1.2824	1
2	1.293	0.67789	0.47176	0.36788
3	0.47567	0.24938	0.17355	0.13534
4	0.17499	0.091743	0.063846	0.049787
5	0.064375	0.03375	0.023488	0.018316
6	0.023682	0.012416	0.0086406	0.0067379
7	0.0087122	0.0045676	0.0031787	0.0024788
8	0.003205	0.0016803	0.0011694	0.00091188
9	0.0011791	0.00061816	0.00043019	0.00033546
10	0.00043376	0.00022741	0.00015826	0.00012341

4 Results and Discussion

This study investigates the approximate solutions for two homogeneous nonlinear TFGDEs using the TPDTM. We have performed all the computational work using MATLAB software. The theoretical and numerical implementation of TPDTM is straightforward, providing a clear insight into the solution behavior. A comparative analysis against established numerical methods, specifi-

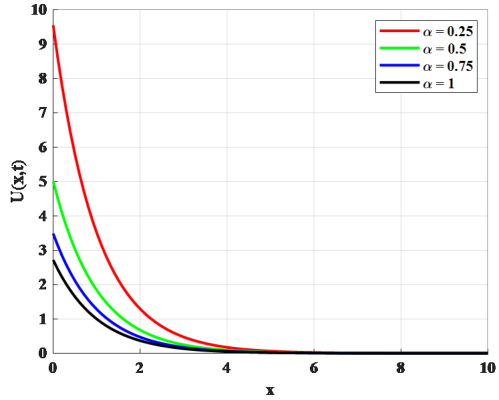

Fig. 2: Analysis of $U(x,t)$ vs. x of test example 1 at different value of $\alpha = 0.25, 0.5, 0.75$, and $\alpha = 1$ with fixed value of $t = 1$ using TPTDM.

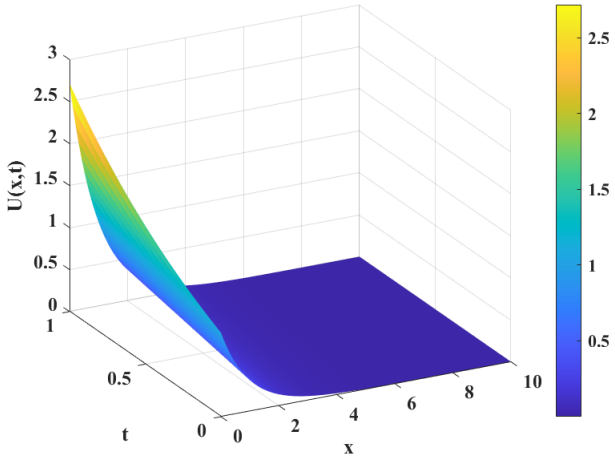

Fig. 3: Analysis of $U(x,t)$ behavior of test example 1 using TPDTM

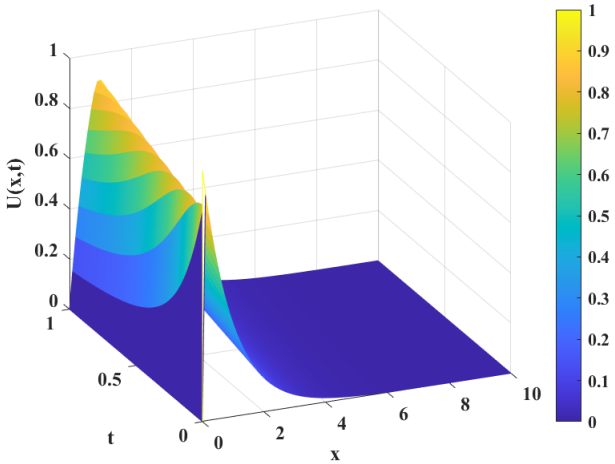

Fig. 4: Analysis of $U(x,t)$ behavior of test example 1 using FDM

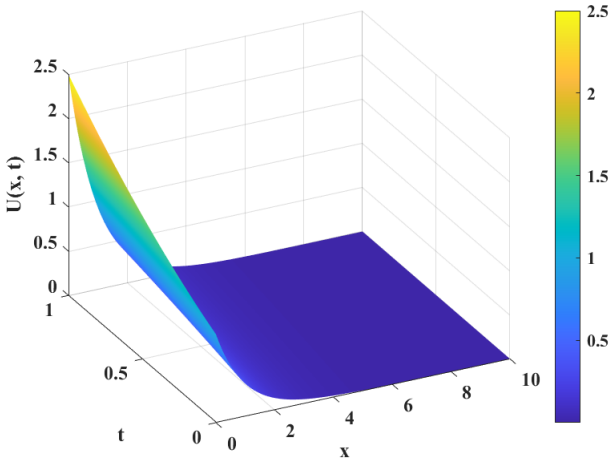

Fig. 5: Analysis of $U(x,t)$ behavior of test example 1 using LADM

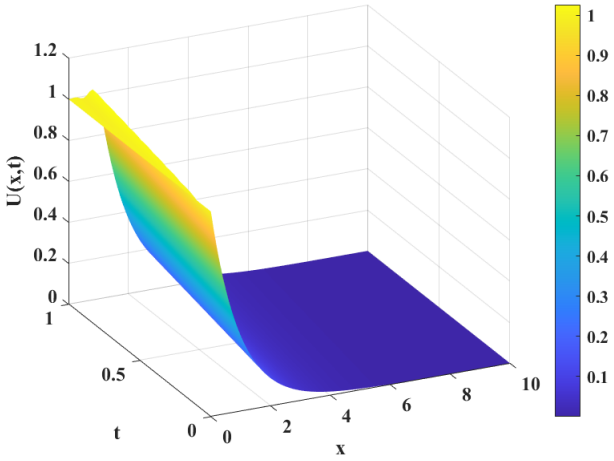

Fig. 6: Analysis of $U(x,t)$ behavior of test example 1 using HPM

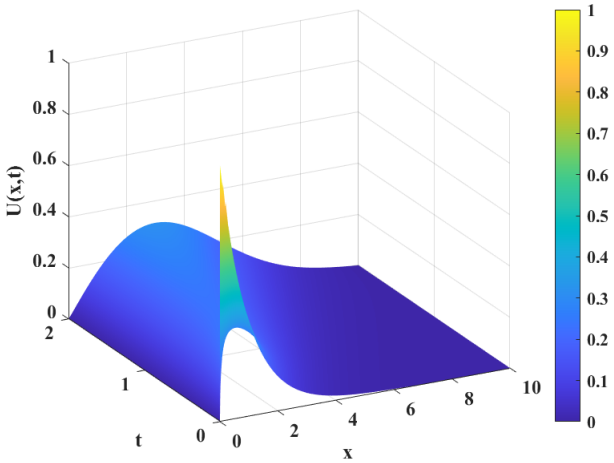

Fig. 7: Analysis of $U(x,t)$ behavior of test example 1 using FEM

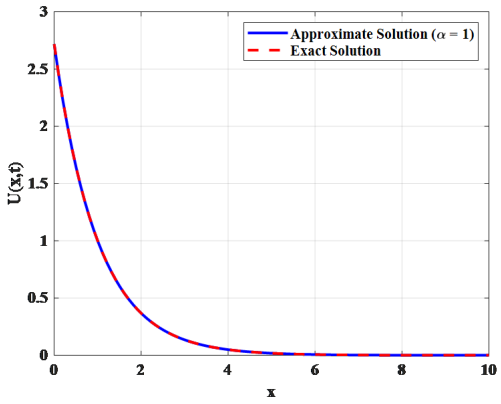

Fig. 8: Illustrative of approximate vs. exact solution of test example 1 at $\alpha = 1$

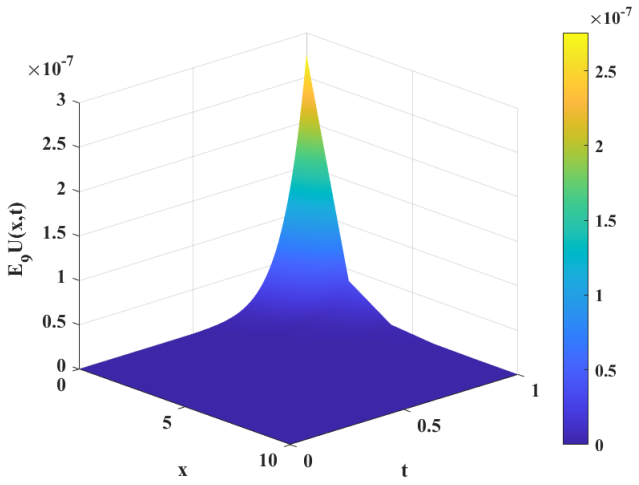

Fig. 9: $E_9U(x,t) = |\text{Exact value} - \text{Approximate value}|$ of test example 1

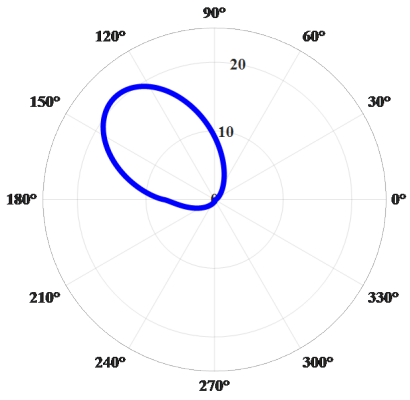

Fig. 10: Polar representation of $U(x,t)$ of test example 1 using TPDTM

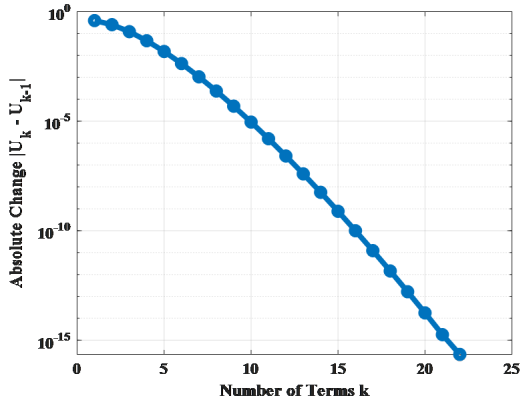

Fig. 11: Convergence behavior of $U(x,t)$ of test example 1 using TPDTM

Table 2: The absolute numerical error $E_kU(x,t)$ calculation to approximate numerical solution of $U(x,t)$ for range of x and t, in the case of test example 1.

k	$E_kU(x,t)$ corresponding to various values of x					
	$x=0$	$x=2$	$x=4$	$x=6$	$x=8$	$x=10$
1	0.5	0.067668	0.0091578	0.0012394	0.00016773	2.27e-05
2	0.16667	0.022556	0.0030526	0.00041313	5.591e-05	7.5667e-06
3	0.041667	0.005639	0.00076315	0.00010328	1.3978e-05	1.8917e-06
4	0.0083333	0.0011278	0.00015263	2.0656e-05	2.7955e-06	3.7833e-07
5	0.0013889	0.00018797	2.5438e-05	3.4427e-06	4.6592e-07	6.3055e-08
6	0.00019841	2.6852e-05	3.6341e-06	4.9182e-07	6.656e-08	9.0079e-09
7	2.4802e-05	3.3565e-06	4.5426e-07	6.1477e-08	8.32e-09	1.126e-09
8	2.7557e-06	3.7295e-07	5.0473e-08	6.8308e-09	9.2445e-10	1.2511e-10
9	2.7557e-07	3.7295e-08	5.0473e-09	6.8308e-10	9.2445e-11	1.2511e-11

Table 3: Illustration of $U(x,t)$ of test example 2 for range of α and x when $t=1$

x-value	$U(x,t)$ with respect to the fractional order α			
	$\alpha=0.25$	$\alpha=0.5$	$\alpha=0.75$	$\alpha=1$
0	0.80748	0.84437	0.88275	0.91731
1	1.0766	1.1258	1.177	1.2231
2	1.4355	1.5011	1.5693	1.6308
3	1.914	2.0015	2.0925	2.1744
4	2.552	2.6686	2.7899	2.8992
5	3.4027	3.5582	3.7199	3.8656
6	4.537	4.7442	4.9599	5.1541
7	6.0493	6.3256	6.6132	6.8721
8	8.0657	8.4342	8.8176	9.1628
9	10.754	11.246	11.757	12.217
10	14.339	14.994	15.676	16.289

cally FDM, LADM, HPM, and FEM, has been conducted to evaluate TPDTM's effectiveness. The obtained results are picturized graphically 1-22 in two and three dimensions and in Tables 1-4. Figures 1-11 illustrate results for test example 1, while Figures 12-22 correspond to test example 2. This presentation facilitates a comprehensive visualization and comparison of the results with TPDTM, FDM, LADM, HPM, and FEM. Tables 1 and 3 present

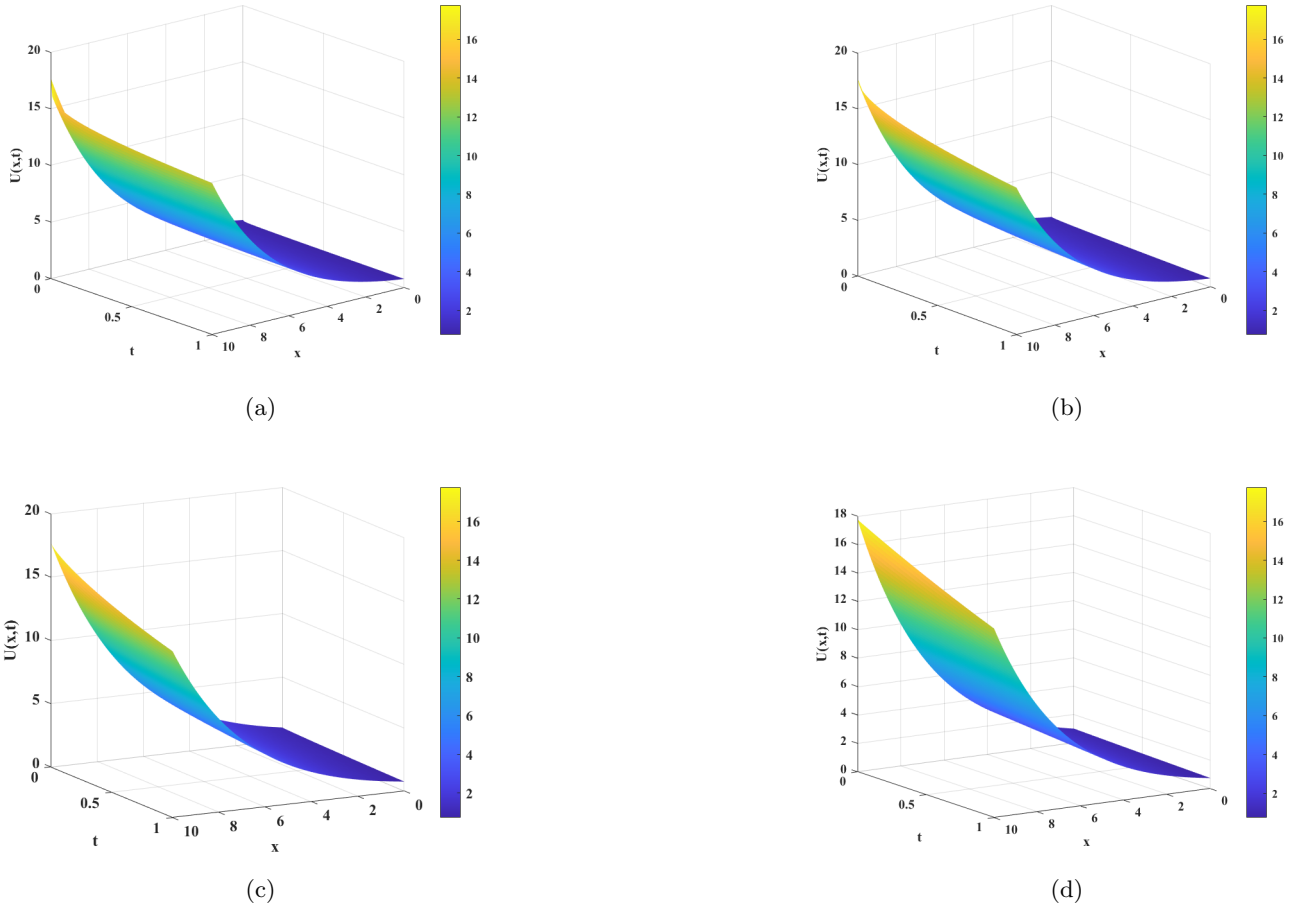

Fig. 12: Analysis $U(x,t)$ of test example 2 is presented for $\alpha = (0.25, 0.50, 0.75$ and $1)$ in a, b, c and d respectively using TPDTM.

Table 4: The absolute numerical error $E_k U(x,t)$ calculation to approximate numerical solution of $U(x,t)$ for range of x and t, in the case of test example 2.

k	$E_k U(x,t)$ corresponding to various values of x					
	$x=0$	$x=2$	$x=4$	$x=6$	$x=8$	$x=10$
1	0.24023	0.96091	3.8436	15.374	61.498	245.99
2	0.055504	0.22202	0.88807	3.5523	14.209	56.836
3	0.0096181	0.038473	0.15389	0.61556	2.4622	9.849
4	0.0013334	0.0053334	0.021334	0.085335	0.34134	1.3654
5	0.00015404	0.00061614	0.0024646	0.0098583	0.039433	0.15773
6	1.5253e-05	6.1011e-05	0.00024404	0.00097617	0.0039047	0.015619
7	1.3215e-06	5.2862e-06	2.1145e-05	8.4579e-05	0.00033832	0.0013533
8	1.0178e-07	4.0712e-07	1.6285e-06	6.514e-06	2.6056e-05	0.00010422
9	7.0549e-09	2.822e-08	1.1288e-07	4.5151e-07	1.8061e-06	7.2242e-06

approximate numerical solutions for the homogeneous nonlinear TFGDEs in test examples 1 and 2, respectively, for various fractional orders $(\alpha = 0.25, 0.50, 0.75, 1)$. The present results are analyzed with Test Example 1 (Figures 1-2, Tables 1) and test example 2 (Figures 12-13, Tables 3) in two and three dimensions.

Figures 1-7 and 12-18 present U(x,t) for the GD equation, obtained using various numerical method such as TPDTM, FDM, LADM, HPM, and FEM. Figures 3-7 (test example 1) and Figures 14-18 (test example 2) further compare U(x,t) obtained using the TPDTM, FDM, LADM, HPM, and FEM. Fig.3 depicts how the gas ve-

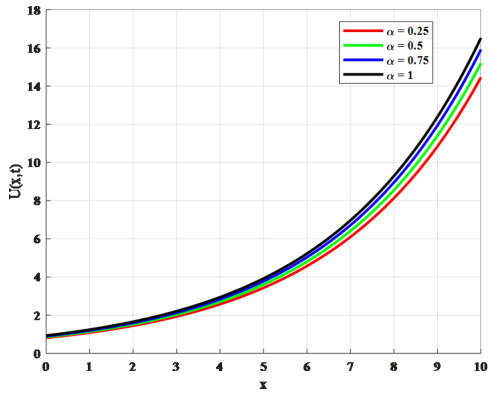

Fig. 13: Analysis of $U(x,t)$ vs. x of test example 2 at different value of $\alpha = 0.25, 0.5, 0.75$, and $\alpha = 1$ with fixed value of $t = 0.30$ using TPTDM.

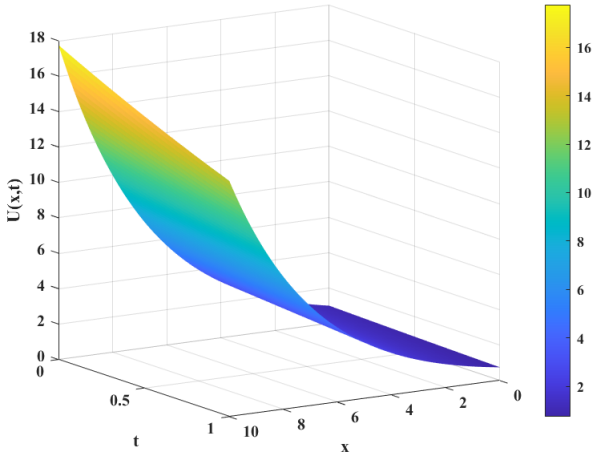

Fig. 14: Analysis of $U(x,t)$ behavior of test example 2 using TPDTM

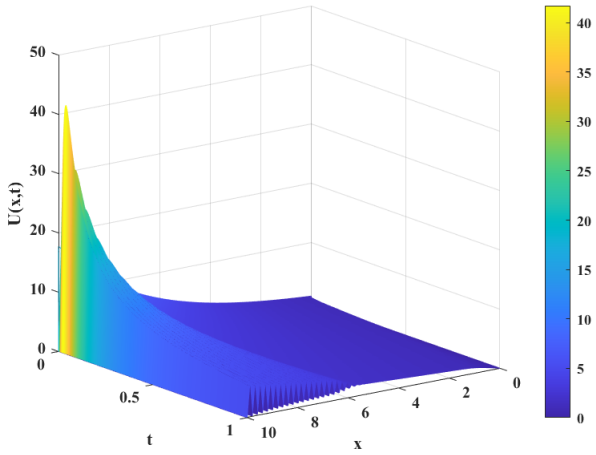

Fig. 15: Analysis of $U(x,t)$ behavior of test example 2 using FDM

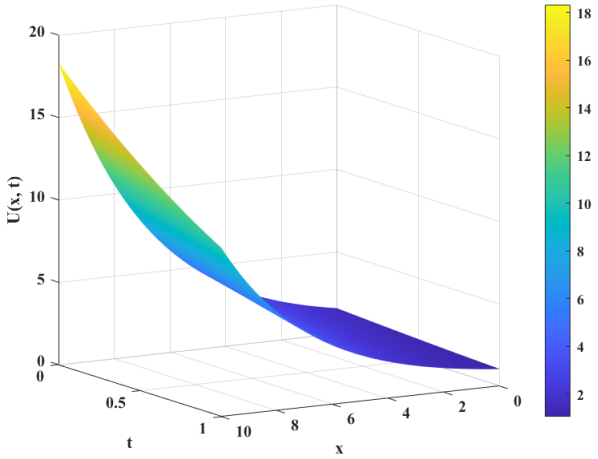

Fig. 16: Analysis of $U(x,t)$ behavior of test example 2 using LADM

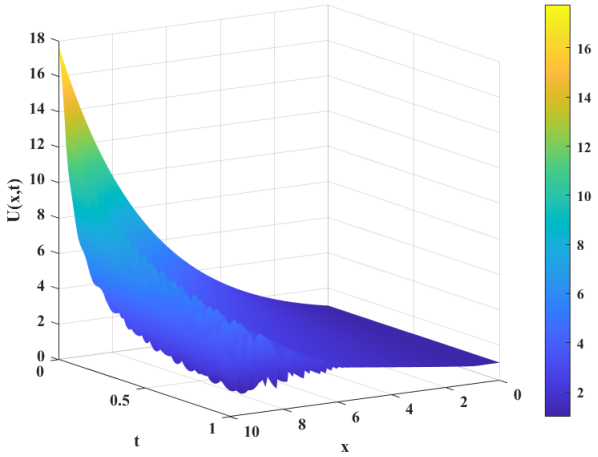

Fig. 17: Analysis of $U(x,t)$ behavior of test example 2 using HPM

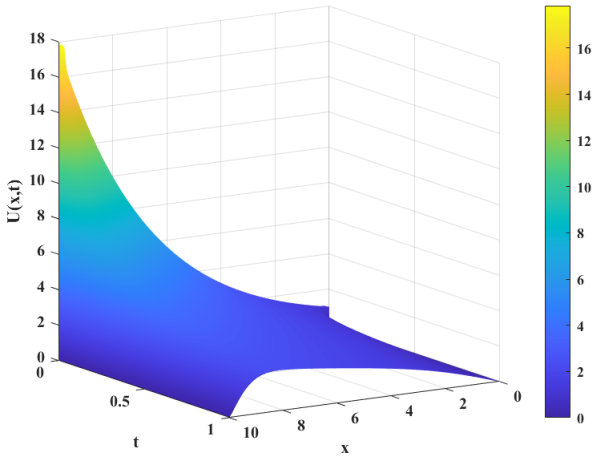

Fig. 18: Analysis of $U(x,t)$ behavior of test example 2 using FEM

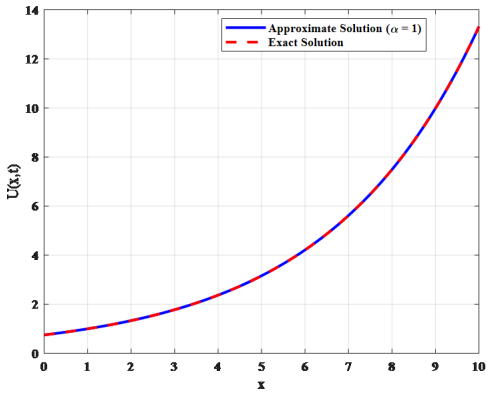

Fig. 19: Illustrative of approximate vs. exact solution of test example 2 at $\alpha = 1$

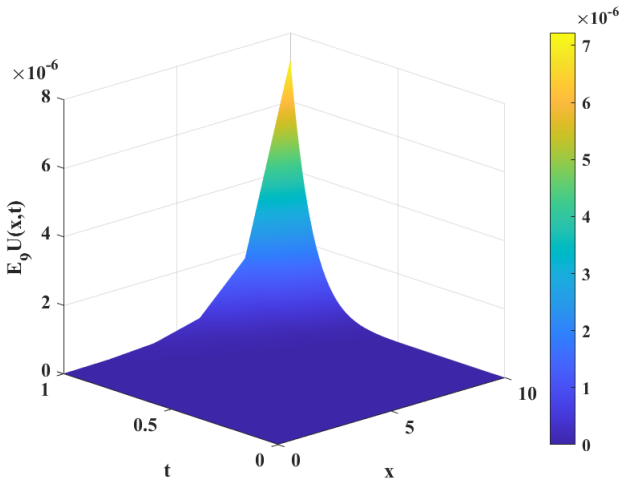

Fig. 20: $E_9U(x,t) = |\text{Exact value} - \text{Approximate value}|$ of test example 2

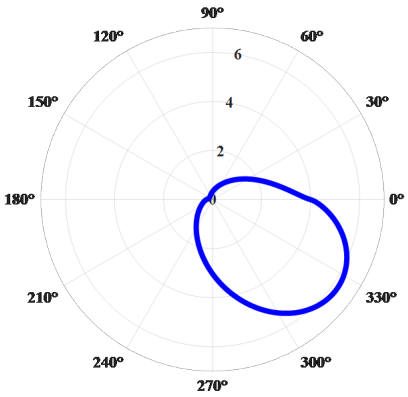

Fig. 21: Polar representation of $U(x,t)$ of test example 2 using TPDTM

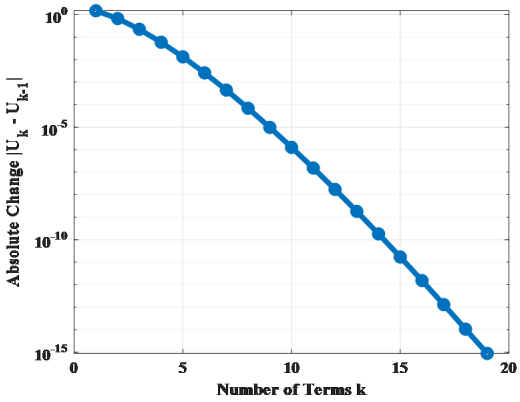

Fig. 22: Convergence behavior of $U(x,t)$ of test example 2 using TPDTM

locity changes over the space x and the time t. The solution shows a strong gradient close to $x = 0$ and decays quickly as x increases. This trend is common in diffusion-dominated flow or shock wave propagation, where the impact of initial conditions decreases with time and distance. The lack of abrupt gradients indicates that the present TPDTM approach well captures the diffusive behavior without causing numerical oscillations. Fig. 4 displays a sharp initial spike close to $x = 0$, which is probably a shock or pulse. As it moves through space and time, it diffuses and decays. The dissipative process of the GD over spatial distance is shown in the sharp decrease in the magnitude of the x-axis. Fig. 5 displays a smooth and fast declining profile, suggesting that the GD start with a strong localized effect that gradually fades across time and space. The lack of abrupt gradients indicates that the method effectively captures the diffusive behavior without causing numerical oscillations. In the Fig. 6, the solution exhibits dissipative gas behavior since it begins at a moderate value and decays smoothly across time and space. This steady, even decrease, indicates that the technique adequately accounts for the system's physical diffusion and damping effects. Fig. 7 indicates a high gradient or initial shock, which is a typical of compressible gas flow, is suggested by the strong peak at low time values. The solution smoothes and decays with time, showing that the initial disturbance has dissipated and that the system has stabilized over time and space.

Fig. 14 shows exponential spatial decay and rapid temporal expansion, indicating that the system dissipates as the spatial variable x grows and evolves with increasing intensity over time, nonlinear wave propagation and shock-like characteristics, which are typical of GD systems with fractional memory effects, are reflected in this behavior. In the Fig.15, strong initial disturbances that eventually fade are indicated by the solution's abrupt initial peak, which decays quickly with time and smoothes out spatially as x grows. Shock wave attenuation or pressure drop propagation, common in GD flows, is reflected in the high initial value followed by a rapid decrease. As shown in Fig. 16, the gradual decline in the solution magnitude over time and space indicates either shock weakening or stable wave energy dissipation. This trend suggests that LADM method effectively captures the GD system's nonlinear diffusion process and decay characteristics. In Fig.17, there are slight oscillations or ripples, particularly close to the lower end of t, the solution exhibits an overall decrease in amplitude over space and time that is compatible with physical dissipation in GD. These oscillations could be a sign of slower convergence of HPM when dealing with substantial nonlinearity in early-time behavior, or they could be numerical errors.

We observed from the Fig. 18 is that the surface shows a quick decline in the velocity over time and space, as is common in dissipative gas flow. The apparent discontinuity close to higher values of x and t points to potential numerical errors with accurately capturing steep gradients using the FEM discretization. TPDTM generates a stable and smooth approximation throughout the computational domain, devoid of oscillations or numerical noise, as seen in Fig. 3 and Fig. 14. Similar graphical representation of solution GD equation with different numerical techniques for text example 1 is existing in literature [33, 34, 35, 36, 37, 38, 39]. The TPDTM proves its superior numerical stability and convergence behavior compared to alternative approaches, especially when space and time scales are varied. The incredible accuracy of TPDTM is shown by the tight adherence of the approximate solution to the theoretical or expected analytical behavior of the GD equation. However, unless extremely precise discretization is employed, techniques like FEM, and FDM may display numerical diffusion or artificial shocks. Compared to conventional discretization-based techniques like FDM and FEM, TPDTM is computationally more economical since it uses fewer terms or iterations to achieve equivalent or better precision. TPDTM manages nonlinear variables methodologically using projection, maintaining the local and global structure of the solution, in contrast to perturbation-based or mesh-based approaches that might have difficulty with

large nonlinearities.

From Figures 3-7 and Figures 14-18, it is evident that the solutions of TPDTM (Figures 3, 14) and LADM (Figures 5, 16) exhibit a high degree of uniformity. In contrast, the solutions derived from FDM (Figures 4, 15), and FEM (Figures 7, 18) show greater fluctuations. Compared to FDM, FEM, HPM (Figures 6, 17) method provides results that are more closely aligned with those obtained through TPDTM and LADM. The comparative analysis indicates that TPDTM and LADM yield smoother and more accurate solution profiles. Notably, TPDTM simplifies the computational process by eliminating the need for polynomial manipulation and integral evaluations, which are required in the LADM technique.

Figures 8 and 19 illustrate that for $\alpha = 1$, the exact and approximate solutions of homogeneous nonlinear TFGDE for test examples 1 and 2, obtained via TPDTM, exhibit a perfect alignment. The minimum errors for different values of x in test example 1 and 2 are tabulated in Tables 2 and 4, providing insights into the stability and convergence of the TPDTM. According to Equation (14) in subsection 2. 8, Tables 2 and 4 indicate that increasing the value of k leads to a decrease in error, signifying that the sequence $\{E_k U(x,t)\}$ is bounded below, it follows that the sequence is convergent, confirming the strong convergence properties of TPDTM.

Furthermore, the error analysis confirms the stability of the solution, as no significant error growth is observed, reinforcing TPDTM's stability. Figures 9 and 20 visualize the magnitude of numerical error of the nineth term of the obtained series for test examples 1 and 2, respectively. Increment in the number of iterations further improves the method's accuracy, demonstrating its effectiveness in solving the problem at hand.

Additionally, we plotted the polar and convergence profile of $U(x,t)$ for test examples 1 and 2, using the TPDTM technique. The polar plots in Figs. 10 and 21 show the solution magnitude $U(x,t)$ or its converted representation in polar coordinates (r,θ), even though the the PDE was initially formulated over a cartesian domain (x,t). Polar curves in both Fig. 10 and Fig. 21 are not centered, which shows that the solutions behave differently in different directions. The nonlinear term in the GD equation, which breaks radial symmetry and adds anisotropy. The solution exhibits spatial irregularities across the domain, as evidenced by asymmetrical elliptical loop in the plot. This asymmetry is a reflection of the memory and nonlinear effects that are present in the equation because of the fractional derivative D^{α}. From the figure, it is clear that the localized expansion or intensification in particular areas, is common in pattern development, reaction-diffusion systems, and shock wave dynamics. The TPDTM approach yields a stable and consistent solution across all angles, demonstrating numerical robustness, as evidenced by the curve's smooth continuity and absence of sharp spikes (Figs 10 and 21). The size of the solution remains consistent across most directions, confirming that TPDTM preserves boundedness and ensures stability. The TPDTM effectively captures the nonlinear coupling and fractional time memory, which are reflected in the plot's little variations. For early-time approximations, where time-domain memory effects are more critical, the representation provided by TPDTM is incredibly effective. This supports the assertion that TPDTM produces a steady and smooth outcome by highlighting the solution's behavior in a projected space. The exponential convergence in the convergence plots, Figs. 11 and 22, indicates a rapid decline in absolute changes between consecutive terms. Figs. 11 and 22 show that the TPDTM solution achieves rapid convergence with fewer than 20 terms. The error drops below 10^{-14} after about 20 terms in Fig.11 and below 10^{-10} after about 15 terms in Fig.22, demonstrating exceptional numerical accuracy.

So, TPDTM is a very dependable technique for resolving nonlinear fractional PDEs; it reduces the computing costs by achieving speedy convergence with a few terms. The convergence plots in Figs.11 and 22, confirm the theoretical and practical soundness of TPDTM and support its applicability to solve more complex or practical problems.

5 Future scope and Conclusions

In this paper, we proposed TPDTM to resolve the homogeneous nonlinear TFGDEs with physical conditions. Present result analysis reveals that the test examples 1 and 2 using TPDTM closely correspond to the exact solutions, affirming its convergence criterion and computationally efficient while exhibiting remarkable accuracy. Our error analysis confirms rapid convergence of the homogeneous nonlinear TFGDE to its exact solutions, highlighting TPDTM as a stable and robust algorithm. A detailed comparative assessment of TPDTM with well-established traditional methods, such as FDM, LADM, HPM, and FEM, demonstrate that TPDTM requires significantly less computational time for fractional-order derivatives. We observe that, the polar and convergence plots of the approximate solution to test examples by employing the TPDTM confirmed that its theoretical analysis is incredible. The present analysis of this research will be helpful, providing several promising avenues for future experimental and theoretical across multiple domains.

References

[1] H. Jafari, M. Zabihi, M. Saidy, "Application of homotopy-perturbation method for solving gasdynamics equation," *Applied Mathematical Sciences*, vol. 2, no. 48, pp. 2393-2396, 2008.

[2] Kumar, Sunil, Huseyin Kocak, and Ahmet Yıldırım, "A fractional model of gas dynamics equations and its analytical approximate solution using laplace transform," *Zeitschrift für Naturforschung A*, vol. 67, no. 6-7, pp. 389-396, 2012.

[3] M. S. Mohamed F. Al-Malki, Al-Humyani, "Homotopy analysis transform method for time-space fractional gas dynamics equation," *General Mathematics Notes*, vol. 24, no. 1, pp. 1-16, 2014.

[4] M. S. Al-Luhaibi, "New iterative method for fractional gas dynamics and coupled burger's equations," *The Scientific World Journal*, vol. 2015, 153124, 2015.

[5] Esen, Alaattin, Berat Karaagac, and Orkun Tasbozan, "Finite difference methods for fractional gas dynamics equation," *Applied Mathematics and Information Sciences Letters*, vol. 4, no. 1, pp. 1-4, 2016.

[6] M. Tamsir, V. K. Srivastava, "Revisiting the approximate analytical solution of fractional-order gas dynamics equation," *Alexandria Engineering Journal*, vol. 55, no. 2, pp. 867-874, 2016.

[7] A. Akgul, Cordero, and J. R. Torregrosa, "Solutions of fractional gas dynamics equation by a new technique," *Mathematical Methods in the Applied Sciences*, vol. 43, no. 3, pp. 1349-1358, 2020.

[8] H. K. Jassim, M.G. Mohammed, "Natural homotopy perturbation method for solving nonlinear fractional gas dynamics equations," *International Journal of Nonlinear Analysis and Applications*, vol. 12, no. 1, pp. 812-820, 2021.

[9] F. K. Iyanda, "Algorithm analytic-numeric solution for nonlinear gas dynamic partial differential equation," *Engineering and Applied Science Letters*, vol. 5, no. 2, pp. 32-40, 2022.

[10] M. Alaroud, O Ababneh, N. Tahat, S. Al-Omari, "Analytic technique for solving temporal time-fractional gas dynamics equations with Caputo fractional derivative," *AIMS Mathematics*, vol. 7, no. 10, pp. 17647-17669, 2022.

[11] H. B. Jebreen, C. Cattani, "Solving fractional gas dynamics equation using muntz-legendre polynomials," *Symmetry*, vol. 15, no. 11, 2074, 2023.

[12] M. A. Yousif, J. L. G. Guirao, P. O. Mohammed, N. Chorfi, D. Baleanu, "A computational study of time-fractional gas dynamics models by means of conformable finite difference method," *AIMS Mathematics*, vol. 9, no. 7, pp. 19843-19858, 2024.

[13] M. Sadaf, Z. Perveen, G. Akram, U. Habiba, M. Abbas, and H. Emadifar, "Solution of time-fractional gas dynamics equation using elzaki decomposition method with caputo-fabrizio fractional derivative," *Plosone*, vol. 19, no. 5, 2024.

[14] Rabia Noureen, Muhammad Nawaz Naeem, Muhammad Kashif Iqbal, Elkenany, and Muhammad Abbas, "A Numerical Scheme for gas dynamics equation involving caputo-fabrico time-fractional derivative," 2023.

[15] Rabia Noureen, Maryam Asgir, Muhammad Kashif Iqbal, and Muhammad Azeem, "Approximate solution of time-fractional gas dynamics equation using exponential B-spline functions," *Optical and Quantum Electronics*, vol. 57, no. 3, pp. 197, 2025.

[16] Rabia Noureen, Muhammad Kashif Iqbal, Maryam Asgir, Bandar Almohsen, and Muhammad Azeem, "A novel approach to approximate solution of time fractional gas dynamics equation with Atangana–Baleanu derivative," *Alexandria Engineering Journal*, vol. 116, pp. 451-471, 2025.

[17] Rasool Shah, Azzh Saad Alshehry, and Wajaree Weera, "A semi-analytical method to investigate fractional-order gas dynamics equations by Shehu transform," *Symmetry*, vol. 14, no. 7, pp. 1458, 2022.

[18] Ahmed Hassan Kamal, A. A. M. Arafa, S. Z. Rida, M. A. Dagher, and Hamed El-Sherbiny, "An effective comparison with least square method for solving fractional gas dynamic equations," *Frontiers in Scientific Research and Technology*, vol. 7, no. 1, 2023.

[19] J. Singh, D. Kumar, A. Kilicman, "Homotopy perturbation method for fractional gas dynamics equation using Sumudu transform," *Abstract and Applied Analysis*, vol. 2013, no. 1, pp. 934060, 2013.

[20] S. Kumar, M. M. Rashidi, "New analytical method for gas dynamics equation arising in shock fronts," *Computer Physics Communications*, vol. 185, no. 7, pp. 1947-1954, 2014.

[21] J. Biazar, and M. Eslami, "Differential transform method for nonlinear fractional gas dynamics equation," *Inter. J. Phys. Sci*, vol. 6, no. 5, pp. 1203-1206, 2011.

[22] J. Singh, and D. Kumar, "Homotopy perturbation algorithm using laplace transform for gas dynamics equation," *Journal of Applied Mathematics, Statistics and Informatics*, vol. 8, no. 1, pp. 55-61, 2012.

[23] M. Rasulov, T. Karaguler, "Finite difference schemes for solving system equations of gas dynamic in a class of discontinuous functions," *Applied Mathematics and Computation*, vol. 143, no. 1, pp. 145-164, 2003.

[24] K. Hemida, M. S. Mohamed, "Application of the homotopy analysis method to fractional order gasdynamics equation," *Journal of Advanced Research in Applied Mathematics*, vol. 2, no. 1, pp. 39-45, 2010.

[25] M. Bagyalakshmi, and G. SaiSundarakrishnan, "Tarig projected differential transform method to solve fractional nonlinear partial differential equations," *Boletim da Sociedade Paranaense de Matematica*, vol. 38,no. 3, pp. 23-46, 2020.

[26] T. M. Elzaki, and S. M. Elzaki, "The new integral transform "tarig transform" properties and applications to differential equations," *Elixir International Journal*, vol. 38, pp. 4239-4242, 2011.

[27] B. Jang, "Solving linear and nonlinear initial value problems by the projected differential transform method," *Computer Physics Communications*, vol. 181, no. 5, pp. 848-854, 2010.

[28] Abdulhameed Qahtan Abbood Altai, "Theory of Fractional Calculus," IAENG International Journal of Applied Mathematics, vol. 52, no. 3, pp717-724, 2022

[29] S. G. Samko, "Fractional Integrals and Derivatives," *Theory and Applications*, 1993.

[30] M. Caputo, "Elasticity and Dissipation," *SIAM Journal on Numerical Analysis*, Italy, 1969.

[31] D. Loonker, and P. K. Banerji, "Fractional tarig transforms and mittag-leffler function," *Bol. Soc. Parana. Mat.*, Vol. 35, no. 2, pp. 83-92, 2017.

[32] K. Athira, D. Narasimhulu, and P. S. Brahmanandam, "Numerical solutions of time fractional NWS and Burger's equations using the tarig projected differential transform method (TPDTM)," *Contemp. Math.*, vol. 6, no. 3, pp. 2907–2928, 2025.

[33] M. Salih, Elzaki, "Exact solution of nonlinear gas dynamic equation using projected differential transform method," *International Journal of Innovation in Science and Mathematics*, vol. 2, no. 5, pp. 2347-9051, 2014.

[34] H. M. Srivastava, and K. M. Saad, "Some new models of the time-fractional gas dynamics equation," *Adv. Math. Models Appl*, vol. 3, no. 1, pp. 5-17, 2018.

[35] Amit, Prakash and Manoj Kumar, "Numerical method for time-fractional gas dynamic equations," *Proceedings of the National Academy of Sciences, India Section A: Physical Sciences*, vol. 89, pp. 559-570, 2019.

[36] Brajesh Kumar Singh, and Pramod Kumar, "Numerical computation for time-fractional gas dynamics equations by fractional reduced differential transforms method," *Journal of Mathematics and System Science*, vol. 6, no. 6, pp. 248-259, 2016.

[37] Abuteen, Eman, and Asad Freihet, "Analytical and numerical solution for fractional gas dynamic equations using residual power series method," *Proceedings of International Conference on Fractional Differentiation and its Applications (ICFDA)*, Jordan, 2018.

[38] Al-luhaibi, S. Mohamed, and Nahed A. Saker, "An analytical treatment to fractional gas dynamics equation," *Appl. Comput. Math*, vol. 3, no. 6, pp. 323-329, 2014.

[39] Olaniyi Samuel Iyiola , "On the solutions of nonlinear time-fractional gas dynamic equations: an analytical approach," *Int. J. Pure Appl. Math*, vol. 98, no. 4, pp. 491-502, 2015.

• Mrs. Athira K was born at Tholambra (Village), Thalassery (Taluk), Kannur (District), Kerala (State), India. Mrs. Athira K received a B.Sc. degree (2016) in Mathematics from Pazhassi raja NSS Collage Mattannur, Kannur University, India; an M.Sc. degree (2018) in Mathematics from Kannur University Campus, Mangattuparamba, India. She is a full-time research scholar and a senior Research Fellow (SRF) in the Department of Statistics and Applied Mathematics, Central University of Tamil Nadu, Thiruvarur-610005, India. She received the UGC-Savitribai Jyotirao Phule Fellowship for Single Girl Child (SJSGC). Her research area is on differential equations, fluid dynamics, fractional differential equations, and magnetohydrodynamics.

• Dr. Narsimhulu D was born at Pallivooru (Village), Vajarapokotturu (Mandal), Srikakulam (District),

Andhra Pradesh (State), India. Dr. Narsimhulu D received a B.Sc. degree (2007) with MPC group from Andhra University, Vishakaptnam, Andhra Pradesh, India; an M.Sc. degree (2009) from Pondicherry Central University, Puducherry, India; and a Ph.D. degree (2018) from BITS Pilani, Hyderabad Campus, Telangana, India. He became a member of the IAENG Society in 2018. His primary research interests lie in applied mathematics, particularly in the area of nonlinear PDEs related to CFD applications. He is presently serving as an Assistant Professor in the Department of Statistics and Applied Mathematics at Central University of Tamil Nadu (CUTN), Thiruvarur-610005, India. Before joining CUTN, he held positions such as Assistant Professor at NIT Andhra Pradesh and GITAM Hyderabad Campus, Teaching Assistant at BITS Pilani-Hyderabad Campus, and Lecturer at Vandana Junior and Degree College, Hyderabad.

His research area is inherently interdisciplinary, integrating mathematical analysis, numerical methods, and scientific computing to address complex problems within the domains of fluid dynamics, gas dynamics, compressible fluid flow, shock waves, magnetohydrodynamics, fractional fluid mechanics, and mathematical biology.

Dr. Narsimhulu is a lifetime member of the Indian Mathematical Society (IMS) in 2013, Forum for Industrial and Applied Mathematics (FIAM) in 2022, Ramanujan Mathematical Society (RMS) in 2022, and Institute of Researchers (InRes) in 2022. He received a gold model during his postgraduate studies and was also awarded the INSPIRE Fellowship (IF110071) by the Department of Science and Technology (DST), New Delhi, in recognition of his excellent academic performance and potential to pursue a research career in Mathematics.